A comparative analysis of Ag and Cu heat sink layers in $L1_0$-FePt films for heat-assisted magnetic recording

Robert Fernandez,[1,a)] Desalegne Teweldebrhan,[2] Chen Zhang,[1] Alexander Balandin,[2] and Sakhrat Khizroev[1]

[1]*Center for 3-D Electronics, Department of Electrical Engineering, University of California—Riverside, Riverside, California 92521, USA*

[2]*Nano-Device Laboratory, Department of Electrical Engineering and Materials Science and Engineering Program, University of California—Riverside, Riverside, California 92521, USA*

(Presented 17 November 2010; received 31 August 2010; accepted 9 December 2010; published online 11 April 2011)

The magnetic properties, structural properties, and thermal conductivity of FePt films deposited on Ag and Cu heat sink layers designed for use in heat-assisted magnetic recording (HAMR) were investigated. It has been found that FePt films grown on Cu have a well-defined $L1_0$-FePt (001) texture while the FePt films grown on Ag appear to be more isotropic. As the thickness of the heat sink layer increases from 15 to 120 nm the coercivity of the FePt films decreases from 1.7 to 1.5 T for Cu and from 1.3 to 1.0 T for Ag. The thermal conductivity measurements, carried out with the "laser-flash" technique, revealed that the overall thermal resistance of the examined structures is dominated by the thermal boundary resistance and the interface effects. The increase in the thickness of Ag and Cu heat sink layers does not lead to the higher *effective* thermal conductivity of the layered structure in the cross-plane direction. The obtained results are important for optimization of the FePt-based structures for HAMR. © *2011 American Institute of Physics*. [doi:10.1063/1.3564968]

Heat-assisted magnetic recording (HAMR) has the potential to increase the areal density beyond the limitations of conventional perpendicular magnetic recording.[1,2] In HAMR, the recording media is heated near its Curie temperature during the writing process and needs to cool down quickly to avoid thermal destabilization of adjacent tracks. Furthermore, the bit transition length depends on the thermal gradient of the media along with the magnetic field gradient.[3–6] Also, the high temperatures associated with HAMR can affect other aspects of the device.[7–9] Therefore, a rapid cooling rate is critical to achieve a sharp bit transition. This leads to an important trade-off between fast heating and rapid cooling, which can be tuned with the use of a heat sink layer.

$L1_0$-FePt thin films are a promising candidate for HAMR media due to its high magnetic anisotropy.[10] For a heat sink layer to be incorporated into FePt HAMR media, the material should demonstrate high thermal stability as well as a compatible crystalline structure for the $L1_0$-phase FePt. Both Ag and Cu are well-known as heat sink materials in electronic devices. Studies have shown that Ag and Cu have similar crystal structures when they are sputter deposited.[11] At the same time, it is well-known that the thermal conductivity of thin films may differ substantially from that of bulk crystals.[12] It is affected by the electron (in metals) or phonon (in semiconductors) boundary or interface scattering, grain size, dislocation lines, quality of the interface, possible alloying, and interdiffusion.[13] For this reason, it is important to investigate the thermal conductivity of the FePt-based thin film structures for HAMR applications. The knowledge of the thermal resistance of the layered magnetic structures and its dependence upon the material choice layer thickness would allow for the structures' optimization for heat-assisted magnetic recording.

In this work we investigate the magnetic properties, structural properties, and thermal conductivity of FePt films deposited on Ag and Cu underlayers. We correlate the magnetic properties with the thermal properties of the structures and assess the feasibility of application of Ag and Cu underlayers as heat sink layers for HAMR.

The structure of the films was Si/Ag or Cu/Ta (2 nm)/CrRu (25 nm)/MgO (2 nm)/FePt (5 nm) prepared by rf (MgO layer) or dc (all other layers) magnetron sputtering. The Ag and Cu heat sink layers were deposited at room temperature with 3 mTorr sputter pressure. The thickness of the heat sink layer was varied at 15, 30, 60, and 120 nm. The Ta layer was deposited at room temperature with a sputter pressure of 10 mTorr, while the CrRu layer was deposited at 300

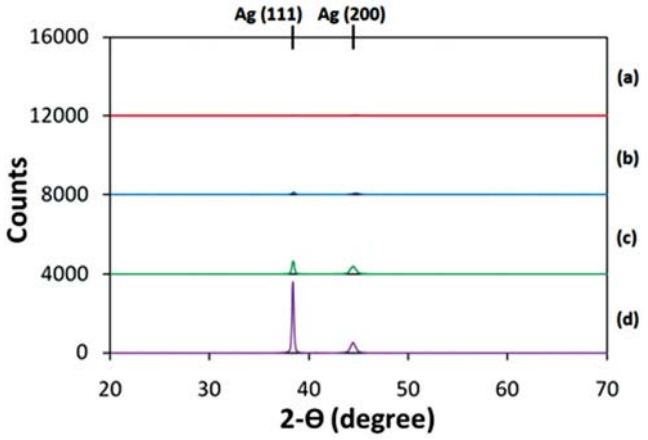

FIG. 1. (Color online) XRD spectra of FePt thin films grown on a Ag heat sink layer of (a) 15, (b) 30, (c) 60, and (d) 120 nm.

[a)]Author to whom correspondence should be addressed. Electronic mail: rfernandez@ee.ucr.edu.

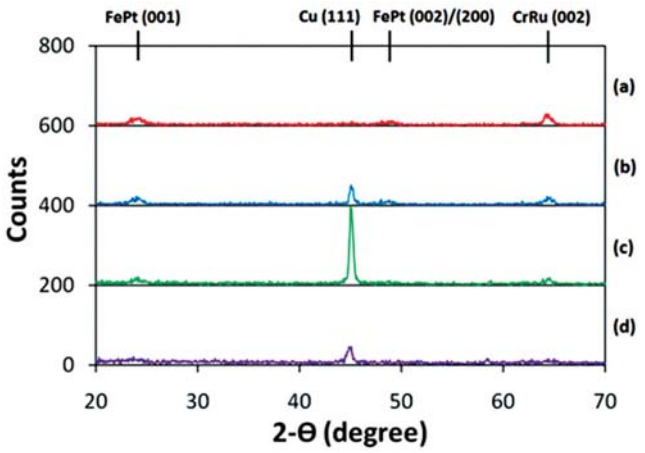

FIG. 2. (Color online) XRD spectra of FePt thin films grown on a Cu heat sink layer of (a) 15, (b) 30, (c) 60, and (d) 120 nm.

°C using 3 mTorr sputter pressure. The samples were cooled to room temperature before depositing the MgO layer at 90 °C and the FePt layer at 550 °C, with 5 and 10 mTorr pressure, respectively. The crystal structure of the films was measured by x-ray diffraction (XRD) while the magnetic properties were measured by a room temperature magneto-optical Kerr effect with an applied field of ±2.7 T.

The thermal conductivity (K) has been measured by the "laser-flash" technique. In this measurement, we directly obtain the thermal diffusivity (α) across the FePt thin films on the Si substrate. After determining the sample's specific heat (C_p) and mass density (ρ) we calculate the thermal conductivity K of the layered sample as $K = \rho\alpha C_p$.

The details of the measurement procedure and comparison of the "laser-flash" method with other measurement techniques have been reported elsewhere by some of us.[14–16] Specifically, we calibrated our experimental procedures using the data obtained with the 3-omega[17] and "hot-disk" techniques.[18,19] One should keep in mind that the actual thermal conductivity of the layers can differ substantially due to size and other effects. The thermal conductivity measured in our experiments should be treated as an *effective* cross-plane value, which characterizes the whole "sandwich" structure rather than individual layers.

Figures 1 and 2 show the XRD patterns of the FePt thin films grown on Ag [Fig. 1] and Cu [Fig. 2] layers with thicknesses of (a) 15, (b) 30, (c) 60, and (d) 120 nm. None of the samples grown on the Ag layer exhibited a FePt (001) texture, while all samples grown on the Cu layer showed a preferred $L1_0$-FePt (001) texture. This is attributed to the fact that the CrRu (002) texture is not formed on the Ag layer, which is necessary to grow the FePt (001) perpendicular orientation. Note also that the samples grown on Ag do not exhibit FePt (111) texture, demonstrating that the FePt films grown on Ag are not perpendicularly oriented nor longitudinally oriented.

The out-of-plane and in-plane hysteresis loops of the FePt films grown on Ag with varying thicknesses are shown in Fig. 3, while the out-of-plane hysteresis loops of the FePt films grown on Cu are shown in Fig. 4. In both cases, the out-of-plane coercivity of the FePt films decreases as the thickness of the heat sink layer increases. For the FePt films grown on Ag, the coercivity decreases from 1.3–1.0 T, while the coercivity decreases from 1.7–1.5 T for the FePt films grown on Cu. For the samples grown on Cu, this decrease in coercivity can be attributed to the fact that as the thickness of the Cu layer increases, both the CrRu (002) and FePt (001) XRD peaks decrease, as seen in Fig. 2. The squareness of the loops of the FePt samples grown on Cu shows a perpendicular orientation, while the squareness of the loops grown on Ag shows that the film is rather isotropic, demonstrated by the fact that both the FePt (001) and FePt (111) peaks are absent in the XRD spectra. The in-plane coercivity of the samples grown on the Ag heat sink layer is also rather large, about 1.5 T, further showing that the samples grown on the Ag heat sink lead to isotropic orientation as opposed to the perpendicular orientation of the samples grown on Cu.

The results of the thermal conductivity measurements are presented in Fig. 5. It shows the thermal conductivity as a function of temperature for the reference Si wafer, and FePt films grown on Ag and Cu layers with thicknesses of

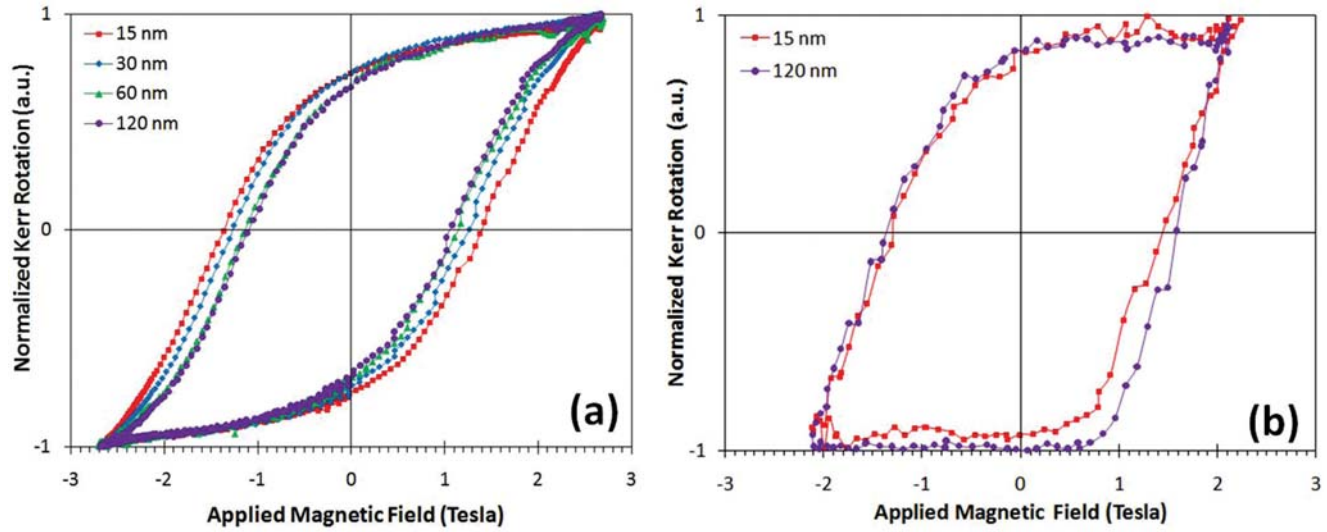

FIG. 3. (Color online) (a) Out-of-plane and (b) in-plane hysteresis loops of FePt thin films grown on a Ag heat sink layer of varying thicknesses.

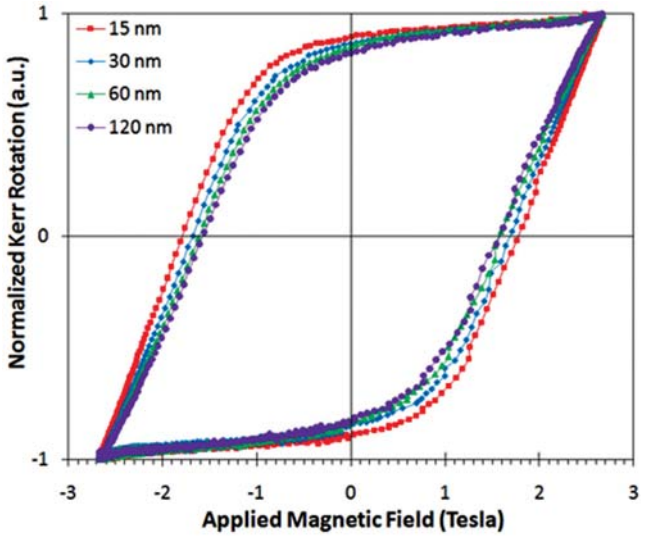

FIG. 4. (Color online) Out-of-plane hysteresis loops of FePt thin films grown on a Cu heat sink layer of varying thicknesses.

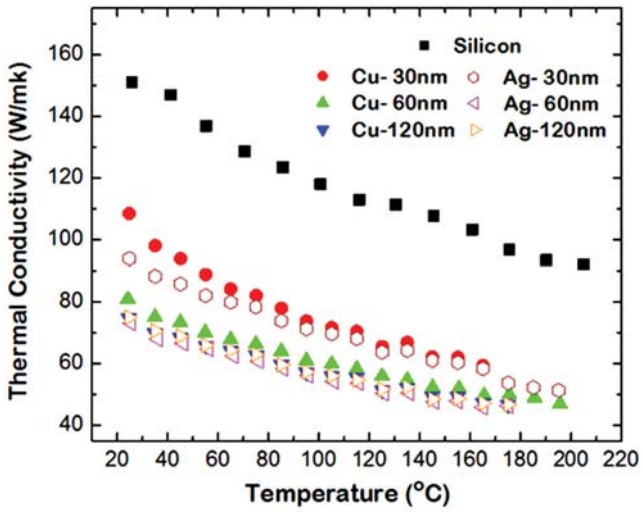

FIG. 5. (Color online) Out of plane thermal conductivity of FePt thin films grown on Ag and Cu heat sink layers of varying thicknesses.

30, 60, and 120 nm. The thermal conductivity of the reference bulk crystalline Si substrate was measured for calibration of the experimental procedure. The measured thermal conductivity of Si closely matches the literature values attesting to the high accuracy of our "laser-flash" technique. The observed dependence of the thermal conductivity K with temperature T (K $\sim$ 1/T) is characteristic for the crystal materials. The measured thermal conductivity of FePt films on Ag and Cu has to be treated as an *effective* thermal conductivity defined for the whole layered structure (including the substrate). Although a portion of the dissipated power can propagate along the layers, the measured values are more closely associated with the *cross-plane* thermal conductivity as determined by the experimental setup and direction of the temperature gradient.

One can see from Fig. 5 that the effective thermal conductivity of FePt layered magnetic structures is rather high (K $\sim$ 80–110 W/mK at RT), which suggests the overall high quality of the layers. It is also related to the high thermal conductivity of Si, Cu, and Ag. Another important observation is the *effective* thermal conductivity does not increase with the increasing thickness of the Cu or Ag layer in the technologically relevant thickness range (30–120 nm). One would expect such an increase in structures with relatively large thicknesses of the individual layers. The situation is different in our multistructures where the layer thickness is in the nanometer range. Our data suggests that the thermal transport in FePt films on Ag and Cu is limited by the thermal boundary resistance (TBR) of the interfaces and nanometer-scale size effects. TBR can be increased in the magnetic layered structure due to possible interdiffusion of the material during the deposition steps, which results in a rougher interface and more scattering for electrons and acoustic phonons. This is an important observation for the thermal optimization of FePt films for HAMR. By controlling the number of interfaces and their quality one can change the thermal resistance of the structure and tune the heating and cooling rates during the recording process.

The overall thermal resistance of the structure can be altered by using substrates with higher thermal conductivity in the desired temperature range[20] or by utilizing lateral heat spreaders.[21,22] The obtained results are important for the thermal design of three-dimensional (3-D) memory and electronic chips.

We acknowledge financial support from the National Science Foundation (NSF) under Contract Nos. 0824019 and 0702752, the NSF/MultiMag3D under Contract No. 0810357, and Department of Defense (DoD)/Defense Microelectronics Activity (DMEA) under Contract No. H94003-04-2-0404-P00002. The work in the Balandin group was supported, in part, by the SRC –DARPA Focus Center Research Program (FCRP) through its Center on Functional Engineered Nano Architectonics (FENA) and DARPA Defense Microelectronics Activity (DMEA) under Agreement No. H94003-10-2-1003.

[1]M. A. Seigler *et al.*, IEEE Trans. Magn. **44**, 119 (2008).
[2]M. H. Kryder *et al.*, Proc. IEEE **96**, 1810 (2008).
[3]T. W. McDaniel, W. A. Challener, and K. Sendur, IEEE Trans. Magn. **39**, 1972 (2003).
[4]A. Lyberatos and J. Hohlfeld, J. Appl. Phys. **95**, 1949 (2004).
[5]F. Akagi, T. Matsumoto, and K. Nakamura, J. Appl. Phys. **101**, 09H501 (2007).
[6]B. Xu *et al.*, J. Magn. Magn. Mater. **320**, 731 (2008).
[7]L. Wu, Nanotechnology **18**, 215702 (2007).
[8]S. J. Greaves and H. Muraoka, J. Appl. Phys. **101**, 09H502 (2007).
[9]B. X. Xu *et al.*, J. Appl. Phys. **103**, 07F525 (2008).
[10]D. Weller *et al.*, IEEE Trans. Magn. **36**, 10 (2000).
[11]A. Zendehnam *et al.*, J. Phys.: Conf. Ser. 61, 1322 (2007).
[12]A. Balandin and K. L. Wang, Phys. Rev. B **58**, 1544 (1998).
[13]W. L. Liu and A. A. Balandin, J. Appl. Phys. **97**, 073710 (2005).
[14]M. Shamsa *et al.*, Appl. Phys. Lett. **89**, 161921 (2006).
[15]S. Ghosh *et al.*, J. Appl. Phys. **106**, 113507 (2009); R. Ikkawi *et al.*, J. Nanoelectron. Optoelectron. **3**, 44 (2008).
[16]D. Teweldebrhan, V. Goyal, and A. A. Balandin, Nano Lett. **10**, 1209 (2010).
[17]W. L. Liu *et al.*, Appl. Phys. Lett. **89**, 171915 (2006).
[18]A. A. Balandin *et al.*, Appl. Phys. Lett. **93**, 043115 (2008).
[19]V. Goyal, D. Teweldebrhan, and A. A. Balandin, Appl. Phys. Lett. **97**, 133117 (2010).
[20]V. Goyal, S. Subrina, D. L. Nika, and A. A. Balandin, Appl. Phys. Lett. **97**, 031904 (2010).
[21]A. A. Balandin *et al.*, Nano Lett. **8**, 902 (2008); S. Ghosh *et al.*, Appl. Phys. Lett. **92**, 151911 (2008).
[22]Q. Shao *et al.*, J. Nanoelectron. Optoelectron. **4**, 291 (2009).